J Mater Sci (2007) 42:5785–5790
DOI 10.1007/s10853-006-0634-2

Synthesis and characterization of thermoplastic polyurethane/montmorillonite nanocomposites produced by reactive extrusion

Yibing Cai · Yuan Hu · Lei Song · Lei Liu · Zhengzhou Wang · Zuyao Chen · Weicheng Fan

Received: 13 March 2006 / Accepted: 28 June 2006 / Published online: 22 March 2007

Abstract The novel polyurethane/montmorillonite (PU/MMT) nanocomposites based on poly (propylene oxide) glycol (POP), 4,4′-diphenymethylate diisocyanate (MDI), 1,4-butanediol (1,4-BD) and MMT has been synthesized using a one-step direct polymerization-intercalation technique by twin-screw extruder. Its structure and thermal properties are characterized by X-ray diffraction (XRD), Transmission electron microscopy (TEM) and High-resolution electron microscopy (HREM), Fourier-transform infrared spectroscopy (FTIR) and Thermogravimetry analysis (TGA), respectively. The results of XRD and HREM analyses show that the silicate layer is well dispersed in PU matrix and this mesostructure can be considered as a delaminated nanocomposites. The TGA analysis indicates that the thermal stability properties of the PU/MMT nanocomposites are increased slightly compared with the pristine PU, due to the increase of the char residue. The mechanical and flammability performances are examined by electronic Universal Tester and Cone calorimetry, respectively. The layered silicate, which acts as a high aspect ratio reinforcement, enhances tensile strength of the PU. Specifically, there is a 25% increase in the tensile strength of PU nanocomposites containing 4 wt.% MMT compared with that of pristine PU. However, the elongation at break of PU/MMT nanocomposites is lower than that of pristine PU. The loading of MMT leads to the remarkably decrease of heat release rate (HRR), contributing to the improvement of flammability performance.

Y. Cai · Y. Hu (✉) · L. Song · L. Liu · Z. Wang · W. Fan
State Key Laboratory of Fire Science, University of Science and Technology of China, Hefei 230026, Anhui, P.R. China
e-mail: yuanhu@ustc.edu.cn

Z. Chen
Department of Chemistry, University of Science and Technology of China, Hefei 230026, Anhui, P.R. China

Introduction

In the recent decade, polymer/layer-silicate nanocomposites have attracted substantial attention of material scientists and manufacturers. Nanocomposites are particle-filled polymers for which at least one dimension of the dispersed particles is in the nanometer range, they have superior physical properties such as thermal, mechanical and barrier properties or some new properties comparing to the original polymer/filler composites [1–6]. Montmorillonite is a kind of natural clay mineral and has a layered structure. It consists of stacked, layered silicate of about 1 nm thickness including two silica tetrahedral sheets sandwiching an edge-shared octahedral sheet of either aluminum or magnesium hydroxide. There are some hydrophilic cations residing in the gallery, such as Na^+ or K^+ ions, which can be exchanged by other cations [7, 8]. The montmorillonite and related layered silicates are the materials of choice for polymer/clay nanocomposites with excellent performances.

Polyurethane is a widely used engineering thermoplastic material with unique properties such as good mechanical, thermal properties, more attention has been given to the synthesis of this family of materials [9–15]. However, the conventional synthesis processing is quite complex and needs rigorous experimental conditions and prolonged times. In generally, the synthesis of polyurethane and its nanocomposites is carried out in flask with abundant solvent, which is not environment friendly. For simplicity, in the present work, we synthesize PU/MMT nanocomposites through a one-step direct polymerization-intercalation

technique by using twin-screw extruder. This kind of synthesis method is very simple both prepared processing and reactive conditions. The potential of industrial manufacture is considerable. The thermal stability, mechanical and flammability properties of the synthesized PU/MMT nanocomposites are also studied compared to that of the unfilled PU. The aim of this article is to synthesize PU/MMT nanocomposites by using the simplest technique and provides a guide to synthesize other polymer-clay nanocomposites.

Experimental

Materials

The pristine montmorillonite (MMT, with a cation exchange capacity of 97 m eq/ 100 g) was kindly supplied by KeYan Company. The polyether used was poly (propylene oxide) glycol (POP), which average molecular weight was about 2000. The 4,4′-diphenylmethane diisocyanate (MDI) and 1,4-butanediol (1,4-BD) were available commercially. The di-2-ethyl-hexyl terephthalate (DOTP) was kindly provided by KeYan Company, which its main function is helpful for the dispersion of the MMT in monomer or prepolymer. All the reactants and solvent were analytic or chemical grade and were used without purification.

Synthesis of the PU and PU/MMT nanocomposites

MMT and POP were placed in a vacuum oven at 120 °C for 12 h to clear out residual water. The PU and its nanocomposites were synthesized with a one-step direct polymerization-intercalation process. The MMT, poly (propylene oxide) glycol (POP), 4,4′-diphenylmethane diisocyanate (MDI) and 1,4-butanediol (1,4-BD) (molar ratio of POP: MDI: 1,4-BD= 1:2:1), DOTP (the mass ratio of DOTP: MMT = 1:5) with appropriate proportion were mixed and stirred vigorously for 3 min at room temperature. Then the mixture was poured into a twin-screw extruder (TE-35, KeYa, JiangShu, China) in the temperature range 180–210 °C, the screw speed is 150 rpm, thus the pristine PU and PU/MMT nanocomposites were obtained. The extruded strands were palletized and dried at 80 °C. The resulting pellets were compressed moulded into sheets (1 and 3 mm thickness) for various measurements. Standard terminology was to add the percentage of clay following the descriptor; i.e., P0 for unfilled PU and P2, P4, P6 for containing 2, 4, and 6 wt.% MMT, respectively.

Characterization

X-ray diffraction(XRD)experiments were performed directly on the samples using a Japan Rigaku D/max-rA X diffraction meter (30 kV,10 mA) with Cu (λ = 1.54Å) irradiation at a rate of 20/min in the range of 1.5–10°.Transmission electron microscopy (TEM) images were obtained on a Jeol JEM-100SX transmission electron microscope with an acceleration voltage of 100 kV. High-resolution electron microscopy (HREM) images were obtained by JEOL 2010 with an acceleration voltage of 200 kV. The TEM and HREM specimens were cut at room temperature using an ultramicrotome (Ultracut-1, UK) with a diamond knife from an epoxy block with the films of the nanocomposite embedded. Thin specimens, 50–80 nm, were collected in a trough filled with water and placed on 200 mesh copper grids.

Infrared spectroscopic experiments on MMT, pristine PU and PU/MMT nanocomposites were performed with a Magna 750 Nicolet Fourier-transform infrared spectroscopy (FTIR). The tensile strength tests were performed with a WD-20D electronic Universal Tester according to ISO527 standard. Samples were made to 25 × 4 × 2 mm size, and the crosshead speed was set at 400 mm/min. For each date point, five samples were tested and the average value was taken.

Thermogravimetry analysis (TGA) was carried out in with a NETZSCH STA 409C thermo-analyzer instrument. In each case, the about 10 mg specimens were heated from 25 to 700 °C using a linear heating rate of 10 °C/min under nitrogen flow.

Flammability was characterized by Cone calorimeter. The signals from the Cone calorimeter were recorded by a computer system. All specimens were prepared by the compression molding into 100 × 100 × 3 mm^3. The samples were examined in a Stanton Redcroft cone calorimeter according to ISO5660 under a heat flux of 35 kW/m^2. Exhaust flow rate was 24L/s and the spark was continued until the sample ignited. The experiments were repeated three times and the results were reproducible to within ±10%. The Cone calorimeter data reported in this paper were the average of three replicated samples.

Results and disscusion

The XRD patterns of MMT and PU/MMT nanocomposites are shown in Fig. 1. The peaks correspond to the (001) plane reflection of the clay, the d_{001} peak of pristine MMT at $2\theta = 5.8°$ corresponds to 1.4 nm interlayer spacing. Fig. 1a–c corresponds to 2, 4, and 6 wt.% contents of MMT in the nanocomposites, respectively. There is the absence of diffraction peaks, indicating the silicate layer are completely exfoliated in the PU matrix and thus form delaminated nanocomposites. To further confirm the dispersion of clay in the PU matrix, electron microscopic measurements are required.

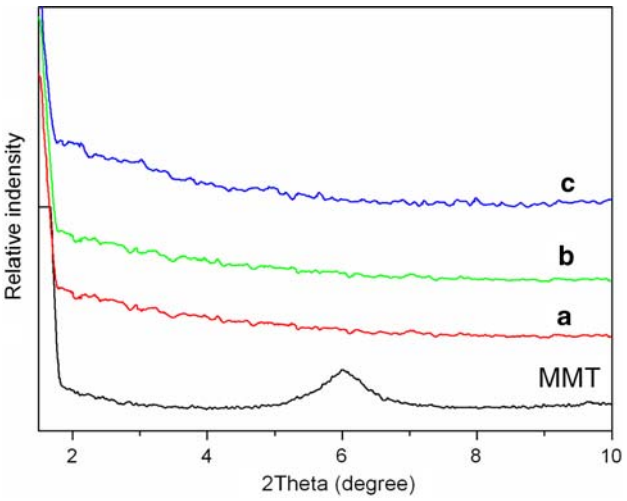

Fig. 1 XRD patterns of MMT and PU/MMT nanocomposites: (**a**) PU/2 wt.%MMT, (**b**) PU/4 wt.%MMT and (**c**) PU/6 wt.%MMT

The TEM image of sample P2 with 2 wt.%MMT at low magnification (Fig. 2a) shows uniform distribution of the silicate layers in the PU matrix, suggesting greater interaction between the silicate particles and the PU matrix. The high magnification morphology of the P2 is also shown by HREM in Fig. 2b. Some single clay platelets with a few multiplayer tactoids are observed in the PU matrix. The clay gallery spacing is about 7–8 nm and this mesostructure can be considered as delaminated nanocomposites, which is again in agreement with the result of XRD.

Figure 3 gives the FTIR spectra of MMT, pristine PU and PU/MMT (P2) nanocomposites. The detailed FTIR band assignment is presented in Table 1. Both pristine PU and PU/MMT have the characteristic bands of polyurethane: 3445, 2940, 2855, 2796, 1732, 1704, 1311, 1223, and 1112 cm^{-1}. The 3329 cm^{-1} peak and 3445 cm^{-1} peak in the IR spectra are N–H in hydrogen bonding and free N–H groups respectively, the formation of hydrogen bonding by C=O group can be determined by examining the peak position at 1732 cm^{-1} for free C=O and 1704 cm^{-1} for hydrogen bonding C=O. Bedsides these bands, PU/MMT (P2) nanocomposites also have the characteristic bands of montmorillonite: 1018, 512, and 460 cm^{-1}, corresponding to the stretching vibration of Si–O–Si, the stretching vibration of Al–O and the Si–O bending vibration of montmorillonite, these indicate the polymer chains have intercalated into the gallery of MMT [11]. In the PU/MMT (P2) nanocomposites, it is found that the positions of peaks for distinctive functional groups are identical with the pristine PU, which means that the segmented structure of PU has not been affected by the presence of MMT [12].

The TGA analysis of the pristine PU and PU/MMT nanocomposites is shown in Fig. 4. Table 2 lists the onset temperature of thermal degradation (T_{onset}, the onset point as 5 wt.% weight loss) and the yield of charred residue at 600 °C. In the temperature range from 275 to 400 °C, the PU/MMT nanocomposites contain assist agent (DOTP) degrades slightly faster than pure polyurethane. This is because the small organic ester molecules tend to degrade before the polyurethane, causing a slight weight loss in the nanocomposites. Meanwhile, it is found that the onset temperature of thermal degradation has more decrease with the MMT loading increase, because the amount of DOTP used increased with the amount of MMT in polyurethane. As a result, the thermal resistance of PU/MMT nanocomposites is lower than that of pristine PU in the first stage. After a complete degradation of the assist agent, the PU/

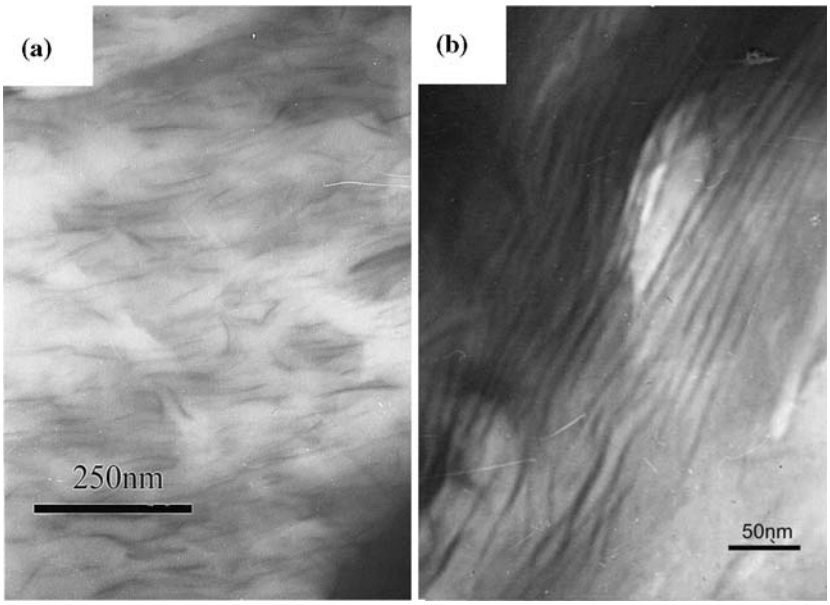

Fig. 2 The TEM and HREM images of PU/2 wt.%MMT nanocomposite

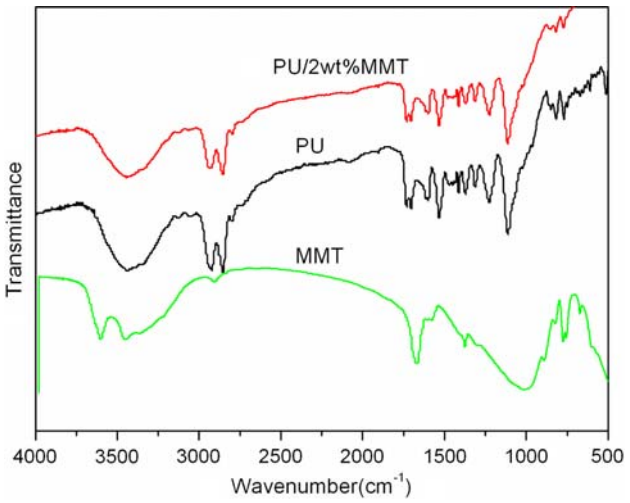

Fig. 3 FTIR patterns of MMT, pristine PU and PU/2 wt.%MMT nanocomposite

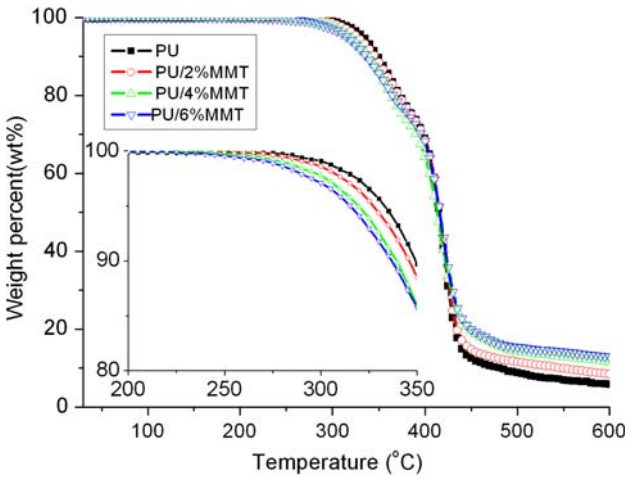

Fig. 4 TGA analysis of the pristine PU and PU/MMT nanocomposites

MMT nanocomposites display higher thermal resistance than that of pristine PU when the temperature range above 400 °C because of the presence of silicate clay. Moreover, the amount of residue is increased with increasing MMT content. The reason is likely to be due to an ablative reassembling of the silicate layers, which may occur on the surface of the nanocomposites. The silicate clay layers act as a superior insulator and as a mass-transport barrier to the volatile products generated during decomposition for increasing the thermal stability. The labyrinth effect of the silicate layers dispersed in the nanocomposites also delays the thermal degradation and enhances the carbonaceous char formation [16–18].

The mechanical properties of the pristine PU and PU/MMT nanocomposites are given in Table 3. In Table 3, the tensile strength of P2 and P4 nanocomposites is higher than that of the pristine PU, indicating that the layered silicate has an enhanced function on the polymeric material. The layered silicate acts as a high aspect ratio reinforcement, similar to fibres within a fibre-reinforced plastic, and therefore enhances the tensile strength of the PU [16]. However, the tensile strength of P6 nanocomposites with 6 wt.% MMT loading has slightly decrease compared with the pristine PU, probably because of the silicate clays with huge surface area and high activity begin to aggregate along with the abundant MMT and result in phase separation between MMT and pristine PU. The elongation at break of the nanocomposites is less than that of the pristine PU and decreases as clay content rises, indicating that the elasticity of PU/MMT nanocomposites decrease when the clay is added, especially the aggregation of MMT with high clay loading in PU matrix is very severe.

Cone calorimeter investigations can be used as a universal approach to ranking and comparing the fire behavior of materials. Therefore, it is not surprising that the cone calorimeter is finding increasing implementation as a characterization tool in the research and development of fire retarded polymeric materials. All materials burning homogeneously under forced flaming conditions in the cone calorimeter with stable flame zone above the surface. Hence, an anaerobe pyrolysis of the polymer was expected. At the end of the test, the flame retardant materials showed minimal flaming along the flame edges, which indicated a delayed burning of the covered materials [19–22]. Cone

Table 1 FTIR band assignment of PU and PU/MMTnanocomposites

Wavenumber	Band assignment
3445 cm^{-1}	N–H stretching vibration
2940 cm^{-1}	Non-symmetric stretching vibration of CH_2
2855 cm^{-1}	Symmetric stretching vibration of CH_2
1732 cm^{-1}	Stretching vibration of C=O
1018 cm^{-1}	Stretching vibration of Si–O–Si
512 cm^{-1}	Stretching vibration of Al–O
460 cm^{-1}	Bending vibration of Si–O

Table 2 Thermal degradation stability of pristine PU and PU/MMT nanocomposites

Sample	T_{onset}(°C)	Weight loss (wt.%) 400 °C	Residue at600 °C (wt.%)	Real residue* at 600 °C (wt.%)
P0	333	30.98	5.85	5.85
P2	327	31.58	8.51	6.87
P4	320	35.54	11.68	8.43
P6	312	33.47	13.96	9.09

* The real residue is that the char for MMT at 600 °C has already been subtracted

Table 3 The mechanical properties of pristine PU and PU/MMT nanocomposites

Samples	Tensile strength (MPa)	Elongation at break (%)
P0	13.0	1421.2
P2	14.7	1390.8
P4	16.3	1332.0
P6	12.3	1230.0

calorimetry is one of the most effective bench-scale methods for studying the flammability properties of materials. Heat release rate, particular peak HRR, has been found to be the most important parameter to evaluate fire safety [23].

The heat release rate (HRR) plots for pristine PU and PU/MMT nanocomposites are shown in Fig.5. The peak HRR values of the pristine PU and PU/MMT nanocomposites are 1121.3 kW/m^2 (P0), 987.6 kW/m^2(P2), 809.8 kW/m^2(P4) and 653.5 kW/m^2(P6), respectively. The peak HRR values of P2, P4, and P6 are about 12, 28, and 42% lower than that of P0, respectively. It is reasonable that as the fraction of silicate clay increases, the amount of carbonaceous char that can be formed increases and the rate of heat release decreases. The HRR decrease of the PU/MMT nanocomposites is due to the barrier property of silicate clay. The results correspond with the TGA analysis. Moreover, it should be noted that the time to ignition of the nanocomposites are both relatively short in comparison with pristine PU. The initial HRR for the nanocomposites are higher than that of the pristine PU at the beginning of combustion. The reason may be the decomposition of small organic ester molecules (DOTP) results in the formation of volatile combustibles in the early stages of nanocomposites combustion, contributing to the combustion. The loading of MMT leads to the decrease of HRR, contributing to the improvement of flammability performance.

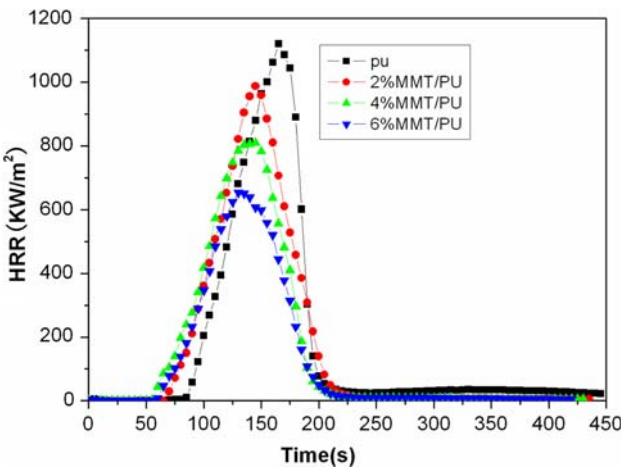

Fig. 5 HRR curves of the pristine PU and PU/MMT nanocomposites

Conclusion

The polyurethane and its nanocomposites are synthesized successfully using a one-step direct polymerization-intercalation reactive extrusion technique. The structure and morphology are characterized by XRD and TEM. The results indicate that the silicate clay is well dispersed in PU matrix and delaminated nanocomposites is obtained. The mechanical, thermal stability and flame retardant properties of PU/ MMT nanocomposites are studied. Although the onset degradation temperature of the PU/MMT nanocomposites advance slightly due to the small organic ester molecules decomposition, the char residue has remarkably increase compared with the pristine PU. Moreover, the amount of the char residue increases with the increasing MMT loadings, contributed to the improved thermal stability. The layered silicate acts as a high aspect ratio reinforcement, similar to fibres within a fibre-reinforced plastic, and therefore enhances the tensile strength of the PU. Specifically, there is a 25% increase in the tensile strength of PU nanocomposites containing 4 wt.% MMT compared with that of pristine PU. The HRR of the PU/MMT nanocomposites has remarkably decrease, contributed to the improvement of flame retardant performance.

Acknowledgements The work was financially supported by the National Natural Science Foundation of China (No.50476026), Specialized Research Fund for the Doctoral Program of Higher Education (20040358056) and Program for New Century Excellent Talents in University.

References

1. Mishra JK, Kim Il, Ha C-S (2003) Macromol Rapid Commun 24:671
2. Tang Y, Hu Y, Wang S (2002) Polym Degrad Stab 78:555
3. Ray SS, Okamoto M (2003) Prog Polym Sci 28:1539
4. Alexandre M, Dubois P (2000) Mater Sci Eng 28:1
5. Carrado KA (2000) J Appl Clay Sci 17:1
6. LeBaron PC, Wang Z, Pinnavaia T (1999) J Appl Clay Sci 15:11
7. Akelah A, Kelly P, Qutubuddin S, Moet A (1994) Clay Miner 29:169
8. Hu Y, Song L, Xu JY, Yang L (2001) Colloid Polym Sci 279:819
9. Penczek P, Frisch KC, Szczepaniak B, Rudnik E (1993) J Polym Sci Polym Chem 31:1211
10. (a) Dearlove TJ et al. J Polym Sci 21 (1977) 1499; (b) Tang W, Frries RJ, Macknight WJ, Eisenbach CD, Macromolecules 55 (1994) 153
11. Zhang X, Xu R, Wu Z (2003) Polym Int 52:790
12. Chen TK, Tien YI, Wei KH (2000) Polym 41:1345
13. Chen TK, Tien YI, Wei KH (1999) J Polym Sci A Polym Chem 37:2225
14. Tien YI, Wei KH (2001) Polym 42:3213

15. Tortora M, Gorrasi G, Vittoria V (2002) Polym 43:6147
16. Song L, Hu Y (2003) Int J Polym Anal Charact 8:317
17. Gilman JW, Jackson CL, Morgan AB, Harris R, Manias E, Gannelis EP (2000) Chem Mater 12:1866
18. Gilman JW, Kashivagi TCL, Gannelis EP, Manias E, Lomakin S, Lichtehan JD et al (1998) In: Le Bras M, Caniino G, Bourbigot S, Delobel R (eds), Fire retardancy of polymers. The Royal Society of Chemistry, Cambridge
19. Schartel B, Bartholmai M, Knoll U (2005) Polym Degrad Stab 88:540
20. Braun U, Schartel B (2004) Macromol Chem Phys 205:2185
21. Schartel B, Braun U, Schwarz U, Reinemann S (2003) Polym 44:6241
22. Schartel B, Braun U (2005) J Fire Sci 23:5
23. Gilman JW (1999) Appl Clay Sci 15:31